

Low Temperature Area Selective Atomic Layer Deposition of Ruthenium Dioxide Thin Films Using Polymers as Inhibition Layers

Nithin Poonkottil, Hannes Rijckaert, Khannan Rajendran, Robin R. Petit, Lisa I. D. J. Martin, Dries Van Thourhout, Isabel Van Driessche, Christophe Detavernier, and Jolien Dendooven*

Area selective atomic layer deposition (AS-ALD) is an interesting bottom-up approach due to its self-aligned fabrication potential. Ruthenium dioxide (RuO_2) is an important material for several applications, including microelectronics, demanding area selective processing. Herein, it is shown that ALD of RuO_2 using methanol and RuO_4 as reactants results in uninhibited continuous growth on SiO_2 , whereas there is no deposition on polymethyl methacrylate (PMMA) blanket films even up to 200 ALD cycles, resulting in around 25 nm of selective RuO_2 deposition on SiO_2 . The excellent selectivity of the process is verified with X-ray photoelectron spectroscopy, X-ray fluorescence, and scanning transmission electron microscopy. AS-ALD is possible at deposition temperatures as low as 60 °C, with an area selective window from 60 to 120 °C. The deposition of RuO_2 using other coreactants namely ethanol and isopropanol in combination with RuO_4 increases the process's growth rate while maintaining selectivity. Testing different polymer thin films such as poly(ethylene terephthalate glycol), (poly(lauryl methacrylate)-*co*-ethylene glycol dimethacrylate), polystyrene, and Kraton reveals an important relationship between polymer structure and the applicability of such polymers as mask layers. Finally, the developed method is demonstrated by selectively depositing RuO_2 on patterned SiO_2 /PMMA samples, followed by PMMA removal, resulting in RuO_2 nanopatterns.

with distinct and promising properties when compared to other transition metal oxides. RuO_2 is well known for its remarkable heterogenous catalysis^[1] and electrocatalysis^[2] capabilities. It is as a very conducting oxide ($\approx 35 \mu\Omega \text{ cm}$) which has comparable resistivity values to ruthenium metal. The chemical and thermal stability of this material adds to its appeal. Furthermore, the scarcity and high cost of ruthenium demands understanding the microscopic properties of RuO_2 .^[3] RuO_2 thin films offer a wide range of applications in large-scale integrated circuits due to its low resistivity, excellent diffusion barrier properties, high temperature stability, and chemical corrosion resistance.^[4,5] RuO_2 is also used as a seed layer for copper deposition, alongside Ru.^[6,7] It has an even better etching capacity than Pt, meaning that RuO_2 can be easily patterned with the help of reactive ion etching (RIO) in O_2/CF_4 discharges.^[8] Recently, it has been also shown that RuO_2 could serve as an excellent barrier layer for Ru diffusion in next-generation Ru based interconnects.^[9]

1. Introduction

Ruthenium dioxide (RuO_2) is a fascinating material with numerous applications. It is the most stable ruthenium oxide,

Atomic layer deposition (ALD)^[10–12] is a vapor phase thin film technique where chemical precursors and coreactants are alternatively pulsed into the reactor and react with the surface in a self-saturated manner. This opens up a plethora of interesting

N. Poonkottil, R. R. Petit, L. I. D. J. Martin, C. Detavernier, J. Dendooven
 Department of Solid State Sciences
 COCOON
 Ghent University
 Krijgslaan 281/S1, Ghent B-9000, Belgium
 E-mail: jolien.dendooven@ugent.be

H. Rijckaert, I. Van Driessche
 Sol-Gel Centre for Research on Inorganic Powders and Thin Films
 Synthesis (SCRIPTS)
 Department of Chemistry
 Ghent University
 Krijgslaan 281 (S3), Ghent 9000, Belgium
 K. Rajendran, D. Van Thourhout
 Photonics Research Group
 Ghent University-imec
 Technologiepark-Zwijnaarde 126, Ghent 9052, Belgium

 The ORCID identification number(s) for the author(s) of this article can be found under <https://doi.org/10.1002/admi.202201934>.

© 2023 The Authors. Advanced Materials Interfaces published by Wiley-VCH GmbH. This is an open access article under the terms of the Creative Commons Attribution License, which permits use, distribution and reproduction in any medium, provided the original work is properly cited.

DOI: 10.1002/admi.202201934

properties such as angstrom level control over film thickness and conformal deposition onto high aspect ratio structures.^[13,14] As a result, ALD has emerged as a key technology in semiconductor manufacturing. Area selective ALD (AS-ALD) is an area that is rapidly emerging, owing to its immense potential in nanomanufacturing. AS-ALD significantly reduces the number of processing steps involved in device manufacturing. Most importantly, it allows deposition on specific areas and thereby leading to self-aligned device fabrication, without compromising the precise thickness control, conformality and other properties achieved by ALD.^[15–17]

Many approaches have been introduced to achieve AS-ALD growth such as selective precursor^[18–21] or coreactant adsorption,^[22–24] selective functionalization of the surface using self-assembled monolayers (SAMs)^[25–32] prior to ALD growth and using other inhibitor molecules.^[33–37] The use of SAMs have been successful in achieving AS-ALD of different metals, metal oxides and even selective deposition on chemically similar materials (for, e.g., ZnO ALD on HfO₂ as growth surface and Al₂O₃ as nongrowth surface).^[32,38] Not all SAMs can be deposited in the vapor phase and require solution processing. During deposition, some SAMs experience structural instability inside the ALD reactor.^[39,40] Alternatively, polymer films have also been employed as passivating layers for area-selective growth.^[41,42] Although polymers still require solution processing, they can benefit from easy and quick preparation, primarily by spin coating, whereas defect-free SAM preparation can be difficult and time-consuming.^[43,44] Polymethyl methacrylate (PMMA), one of the most commonly used mask layers for AS-ALD, is also a popular e-beam resist material, and the compatibility with different patterning techniques eases the production of patterned PMMA structures. The polymer coatings can also be easily removed following the AS-ALD process by using a plasma step or dipping in appropriate solvents.^[44] AS-ALD of metal oxides such as Al₂O₃, ZnO, ZrO₂, TiO₂, HfO₂ and metals like Ru, Ir, Rh, and Pt has been demonstrated successfully using polymers as mask layers.^[21,41,42,45,46] However, the AS-ALD of RuO₂ has not been demonstrated before. The ALD of RuO₂ itself using metalorganic precursors in combination with O₂ gas is challenging as reported by Aaltonen et al.^[47] The (sub) surface O₂ is used mainly for the combustion of organic ligands adsorbed during the next pulse, such that Ru films are formed instead of

RuO₂ films. This introduces the need for higher O₂ partial pressures to achieve pure RuO₂ films. In this context, we recently reported an ALD process for RuO₂ using RuO₄ and alcohols as reactants.^[48] In our case, alcohols act as reducing agent that reduces the RuO₂ partially, facilitating the nucleation of RuO₄ and additional deposition of RuO₂ in the subsequent pulse.

Although there exist some reports on area selective deposition of metallic Ru, no reports on RuO₂ have been published. Owing to the important properties RuO₂ offers, especially in microelectronics, it is important to investigate and develop feasible area selective deposition protocols for this material. Hence, in this work, we demonstrate AS-ALD of RuO₂ at deposition temperatures as low as 60 °C. The selective deposition is achieved on SiO₂, whereas no deposition was observed after 200 cycles on blanket PMMA wafers. The process was found to be inherently selective, leading to deposition of RuO₂ as thick as 25 nm on SiO₂ without any deposition on PMMA. In order to expand the library of polymer materials that can be used as mask layers for AS-ALD, we examined the growth of RuO₂ on different polymers such as polyethylene terephthalate glycol (PET-G), poly(lauryl methacrylate)-co-ethylene glycol dimethacrylate (PLMA-co-EGDMA), polystyrene (PS), and kraton. It was found that PMMA like polymers (in the sense that C=O bond is present) such as PLMA-co-EGDMA (block copolymer of PLMA and EGDMA) and PET-G did not yield any RuO₂ growth whereas on PS and Kraton, RuO₂ growth was observed. Thus, an important relationship was obtained that polymers with C=O groups could be used as mask layers, whereas aromatic C=C containing polymers cannot be. Finally, area selective RuO₂ is successfully demonstrated on a patterned SiO₂/PMMA wafer as a proof of concept. An acetone dip can be used to remove the unreacted PMMA in the next stage, resulting in RuO₂ nanostructures on SiO₂. The method is relatively simple and straightforward due to the low processing temperature and due to the fact that PMMA or PMMA like polymers can be used as a mask layer.

2. Results and Discussion

Figure 1 depicts the various steps involved in the area selective deposition of RuO₂ thin films using PMMA as an inhibition

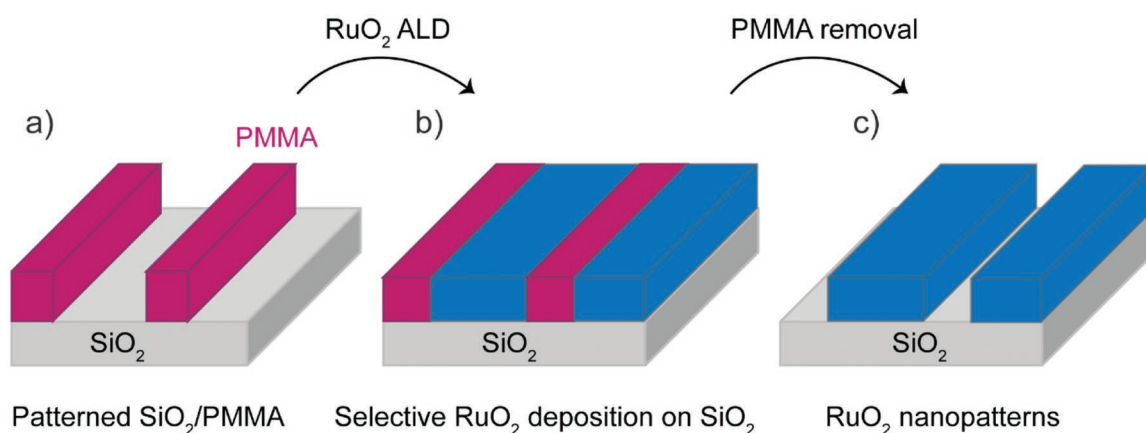


Figure 1. Schematic overview of the developed area selective RuO₂ ALD approach.

layer. We use a recently developed RuO₂ ALD process from our group for this purpose. As previously reported, RuO₄ is used as a Ru source, and the RuO₄-methanol based RuO₂ ALD process grows on silicon substrates with a growth per cycle (GPC) of ≈1 Å per cycle.^[48] We discovered that performing the same process on PMMA blanket wafers does not result in RuO₂ deposition. This difference in reactivity is being investigated further in order to achieve AS-ALD of RuO₂. Starting with a patterned SiO₂/PMMA wafer, RuO₂ should be deposited selectively on SiO₂, leaving the PMMA unreacted (step b). Finally, once the desired thickness of RuO₂ has been achieved, the unreacted PMMA can be easily removed by performing an additional plasma step or acetone dip to create RuO₂ nanostructures on the growth surface.

2.1. Selectivity: SiO₂ versus PMMA

The selectivity between the growth and nongrowth surfaces is an important aspect in AS-ALD, requiring insights on how many ALD cycles can be performed before the selectivity is lost. To assess the selectivity of the RuO₂ ALD process, it was first performed on SiO₂ (silicon with native oxide) and PMMA (120 nm, spin coated) blanket wafers. At a substrate temperature of 100 °C, different ALD cycles of the RuO₄-methanol process were performed on these substrates. The Ru L α X-ray fluorescence (XRF) counts on these samples were investigated after the depositions. **Figure 2a** shows that even after 200 ALD cycles, there is no evidence of Ru on the PMMA blanket wafer (absence of Ru peak in XRF spectra). On the other hand, a clear Ru XRF signal was present on SiO₂, and it increased linearly with ALD cycle number, as is typical for most metal oxide ALD processes. The thickness of RuO₂ deposited on SiO₂ was measured using X-ray reflectivity (XRR, raw spectrum shown in Figure S1, Supporting Information), and a GPC of ≈1.1 Å per cycle was obtained, which is consistent with our previous work. The XRR data confirmed that ≈24 nm RuO₂ (Figure 2a, right γ -axis) can be deposited on SiO₂ without any deposition

on PMMA, opening up the possibility of area selective RuO₂ deposition using SiO₂/PMMA patterned wafers, as discussed in Figure 1. The films were amorphous as deposited on SiO₂, but they can be crystallized into rutile RuO₂ by annealing in helium or air to around 400 °C (Figure S2, Supporting Information).

X-ray photoelectron spectroscopy (XPS) measurements on blanket SiO₂ and PMMA were performed to confirm the selectivity. Figure 2b displays the XPS spectra obtained after 200 ALD cycles at 100 °C substrate temperature. Due to the overlap of the Ru 3d and C 1s peaks in the XPS spectrum, the Ru 3p peak was investigated for both PMMA and SiO₂ samples. Figure 2b clearly shows that even after 200 cycles, there is no evidence of Ru on the PMMA layer. On the other hand, there is a clear presence of Ru signal on SiO₂, demonstrating the area selective nature of our process, which is completely consistent with the XRF results presented. In other words, even after 200 ALD cycles, this process achieved a selectivity value of 1. Note that selectivity is defined as

$$S = \frac{\theta_{GA} - \theta_{NGA}}{\theta_{GA} + \theta_{NGA}} \quad (1)$$

where θ_{GA} and θ_{NGA} represent the amounts of material deposited on the growth and no-growth areas, respectively.^[51]

2.2. Temperature Dependence of Selectivity

Previous AS-ALD reports indicate that deposition temperature is an important factor influencing ALD process selectivity: at low deposition temperatures, ALD process selectivity may be reduced or lost due to adsorption of precursors or other ligand fragments on the nongrowth surface.^[52] Higher temperatures can result in improved selectivity. The same RuO₂ ALD process was repeated on blanket PMMA and SiO₂ wafers at different substrate temperatures to evaluate the temperature dependence on the selectivity of RuO₂ ALD. In short, three different deposition temperatures, 60, 80, and 100 °C, were chosen, and

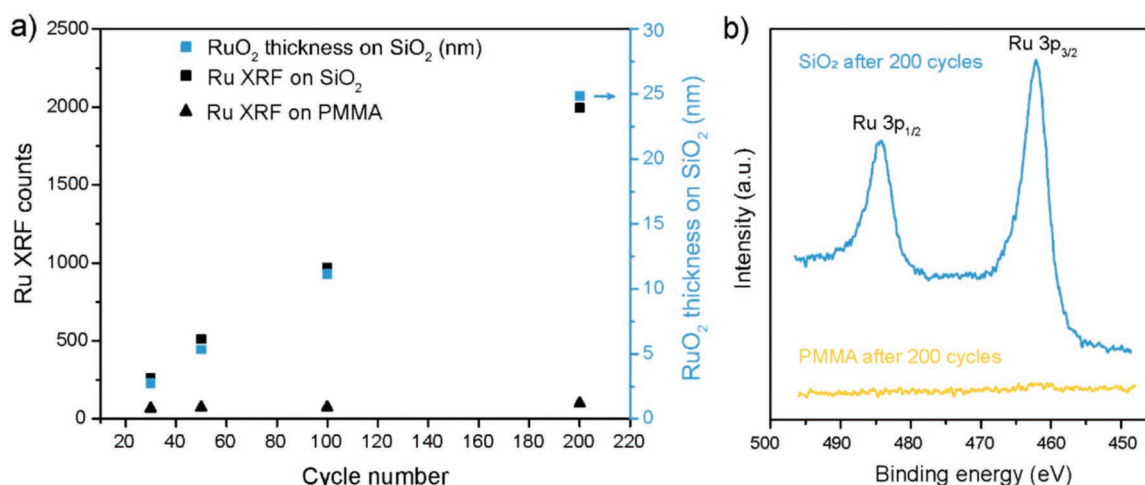


Figure 2. a) Ru XRF counts (left γ -axis) as a function of number of cycles on SiO₂ and PMMA blanket samples and thickness of RuO₂ (right γ -axis) on SiO₂ blanket samples as measured by XRR. b) Ru 3p XPS spectra on SiO₂ and PMMA blanket samples after 200 RuO₂ ALD cycles. The substrate temperature used in this case was 100 °C and the PMMA thickness was 120 nm.

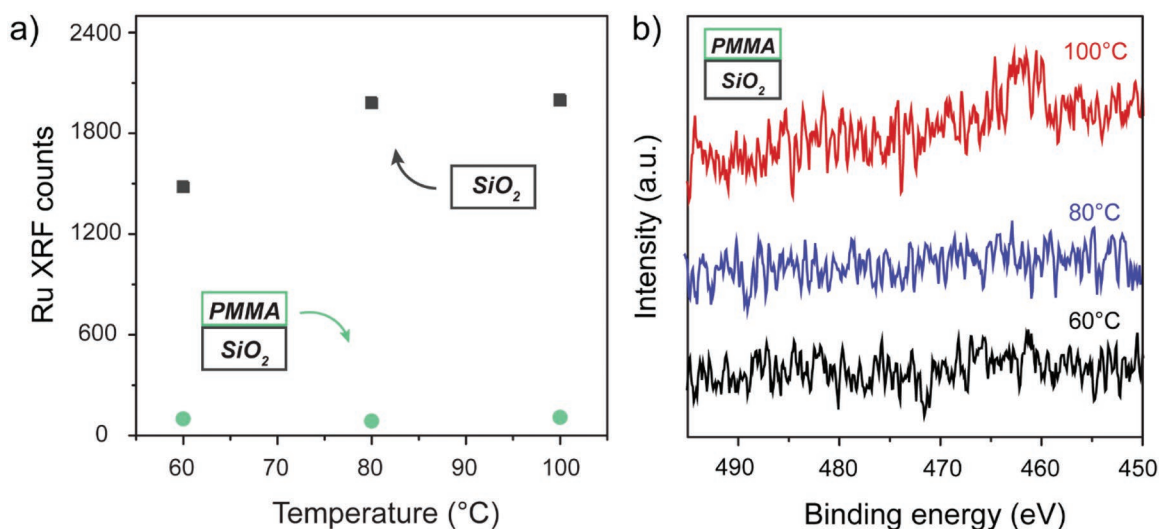


Figure 3. Temperature dependence of selectivity. a) XRF counts on SiO₂ and PMMA after 200 cycles at different substrate temperatures. b) Ru 3p XPS spectra region on PMMA after 200 cycles at different substrate temperatures. The PMMA thickness was 120 nm. The XPS spectra have been given a vertical offset for clarity.

200 cycles of the RuO₂ ALD process were carried out. RuO₄ precursor is known to decompose around 125 °C.^[53]

Following the deposition, these samples were examined using XRF and XPS. **Figure 3a** shows that the Ru XRF signal is not present on PMMA regardless of deposition temperature, whereas a clear signal was observed on SiO₂ blanket samples at all temperatures (Figure S3, Supporting Information). The comparable Ru XRF intensity on SiO₂ at all temperatures investigated indicates a similar growth rate at these various temperatures. The temperature independence of selectivity was confirmed by XPS, where Ru 3p peaks were evaluated (Figure 3b) on PMMA blanket samples. No significant Ru peak was observed at any of the substrate temperatures tested. This implies that process selectivity is not lost even when the substrate temperature is reduced to as low as 60 °C (making the AS-ALD window from 60 to 120 °C), which opens up opportunities to perform area selective ALD on substrates that require lower deposition temperatures, such as flexible substrates.

2.3. PMMA Thickness

It is important to check whether the selectivity holds true if polymer films of other thicknesses are used. AS-ALD suffers from the so-called lateral growth (“mushroom” growth) because of the isotropic nature of ALD processes. Although currently no real solutions exist to overcome this, the use of thicker passivation layers (thicker than the desired coating) has been suggested.^[16,54] Another question to address is if by increasing the polymer thickness, the selectivity is lost due to defects or nucleation of ALD growth on the polymer promoted by the remnants of any precursor diffusing into such a thicker polymer layer. This diffusion (if any) would also complicate the removal of the polymer after the AS-ALD process.^[55,56] To evaluate this, we performed RuO₂ ALD (200 cycles) at 100 °C on spin coated PMMA blanket films of different thicknesses (35, 120, and

300 nm) and studied the Ru 3p peak with XPS. In our case, however, the Ru signals on all of these PMMA samples were negligible, implying that the PMMA thickness has no effect on the selectivity of the developed area selective process (**Figure 4**).

2.4. Other Coreactants

In a previous work, we have demonstrated that different alcohols can be used as coreactants to deposit RuO₂. We discovered that by using a higher alcohol chain coreactant, the growth rate can be increased as well. Specifically, methanol displays a

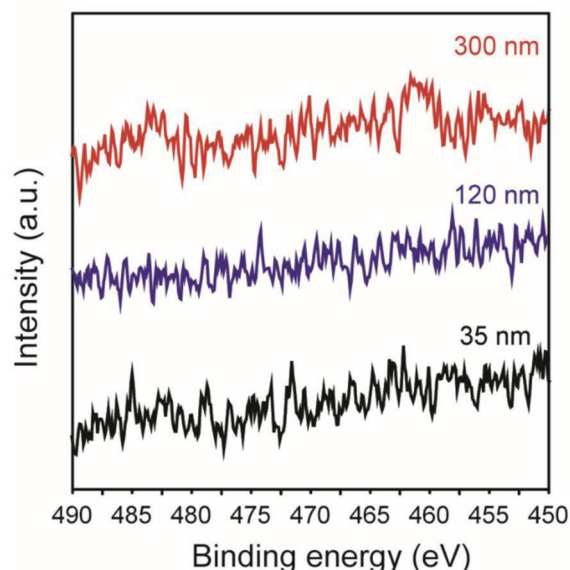


Figure 4. XPS data for Ru 3p signal on different PMMA film thickness, for the RuO₂ ALD performed at a substrate temperature of 100 °C. The XPS spectra have been given a vertical offset for clarity.

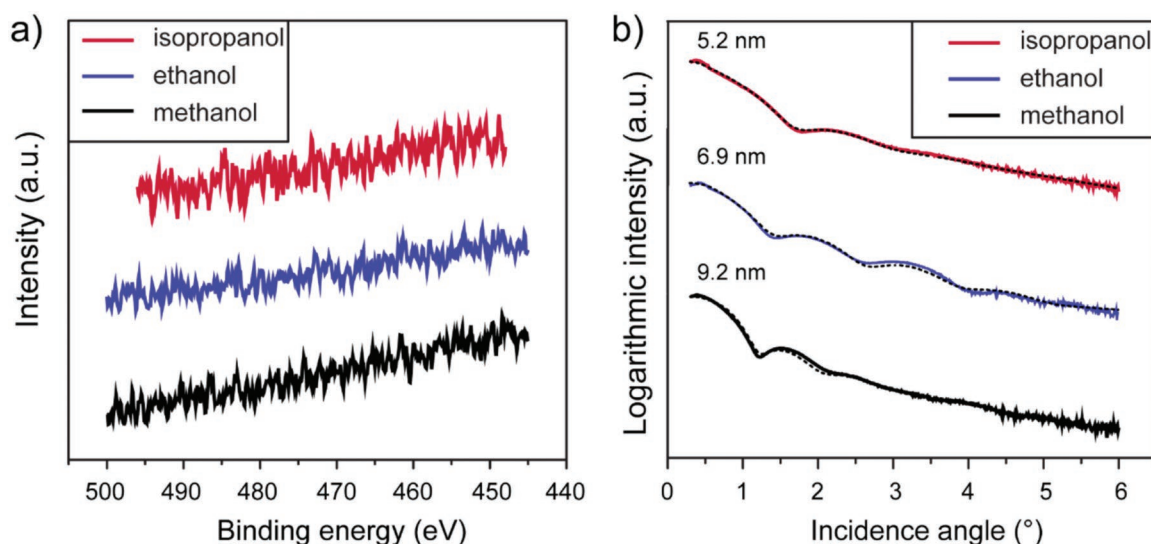


Figure 5. a) Ru 3p XPS spectra after 50 ALD cycles using different coreactants. b) XRR patterns on SiO₂ using different alcohols. The solid and dashed curves indicate measured and fitted data, respectively. The XRR patterns have been given a vertical offset for clarity.

GPC of 1 Å per cycle, ethanol yields a GPC of 1.5 Å per cycle, and 1-propanol and 2-propanol both result in a GPC of around 2 Å per cycle.^[48] However, as previously reported, the properties (crystallinity, conductivity, etc.) of the films prepared by these different alcohols were found to be very similar. We have already demonstrated in this work that the methanol-based process could be used for the AS-ALD of RuO₂. The selectivity of other alcohol-based RuO₂ ALD processes, on the other hand, will be determined by the alcohol's ability to bind to the PMMA surface. If the alcohol is easily bound to PMMA, it is very likely that the selectivity will be lost or reduced. There are reports where AS-ALD is enabled due to selective coreactant adsorption.^[16,23] For example, AS-ALD of Fe₂O₃ was enabled selective O₂ adsorption and dissociation on Pt surfaces rather than oxide surfaces. Similarly, unwanted adsorption of coreactants on a surface might also lead to loss of selectivity. In our case, if the other alcohols bind to the PMMA surface, the RuO₄ molecules can thus react with the alcohol related groups on the surface and thereby the selectivity can also be affected. To evaluate this, we performed three different depositions (50 cycles of methanol, ethanol, and 2-propanol based processes) on blanket PMMA and SiO₂ samples at a deposition temperature of 100 °C to test the selectivity dependence when using different coreactants. The samples were analyzed using XRF (Figure S4, Supporting Information) and XPS to see if any Ru was present on the PMMA layer after deposition. The Ru 3p XPS spectra in **Figure 5a** reveal that no Ru is present on PMMA during any of these three different processes. This means that for at least 50 ALD cycles, any alcohol such as methanol, ethanol, or 2-propanol can be used as a coreactant to deposit RuO₂ selectively on SiO₂ without affecting the PMMA layer. XRR measurements (Figure 5b) indicated that ≈5.2, 6.9, and 9.2 nm RuO₂ films are obtained using methanol, ethanol, and isopropanol, respectively. This suggests that ethanol or 2-propanol could be used to achieve faster growth of RuO₂ on SiO₂ without compromising selectivity as well as significantly reducing experiment duration and Ru precursor consumption.

2.5. Deposition on Other Polymers

We have already shown that PMMA layers can be used to inhibit RuO₂ ALD growth, at the same time allowing selective deposition on SiO₂. The feasibility of deposition of RuO₂ on other polymers is interesting in area selective deposition as this will also broaden the set of polymers that can (or cannot) be used as mask layers for area selective ALD. For this purpose, different polymers such as PS, Kraton, PLMA-co-EGDMA, and PET-G were also studied for RuO₂ growth. PS comes under the family of vinyl polymers. It is a long chain polymer with a phenyl ring attached to every other carbon atom. Kraton polymers are styrene block copolymers that consist of polystyrene blocks and rubber blocks (in our case it was an ethylene and butylene unit in between two polystyrene units). So, both PS and Kraton contain polystyrene units in the structure. PMMA contains two side groups, an ester group and a methyl group. In PLMA-co-EGDMA, the part PLMA is very similar to PMMA expect that the ester CH₃ group is replaced by a large alkyl group and this PLMA part is coupled to EGDMA linkages.

PET-G is similar to PET, but a part of ethylene groups is replaced by cyclohexanedimethylene. In PET-G, the functional group is attached to the main chain instead of the side chain. This allows a systematic study of RuO₂ deposition on different polymers (the structures are provided in **Figure 6a–e**) based on the polymer chain composition, length, and functional groups present. In short, two sets of polymers, one set containing styrene part (PS and Kraton) and the other set containing C=O (PMMA, PLMA-co-EGDMA, PET-G) as functional groups were investigated.

The growth of RuO₂ on these polymers should be dependent on the ability of the RuO₄ molecules to interact with the polymer chain or functional group. XPS analyses revealed that RuO₂ growth occurred on PS and Kraton, as evidenced by a distinct Ru 3p peak (Figure 6f); a SiO₂ reference is also provided for comparison. PMMA, PLMA, and PET-G, on the other hand, showed no growth (absence of Ru 3p peak in Figure 6g).

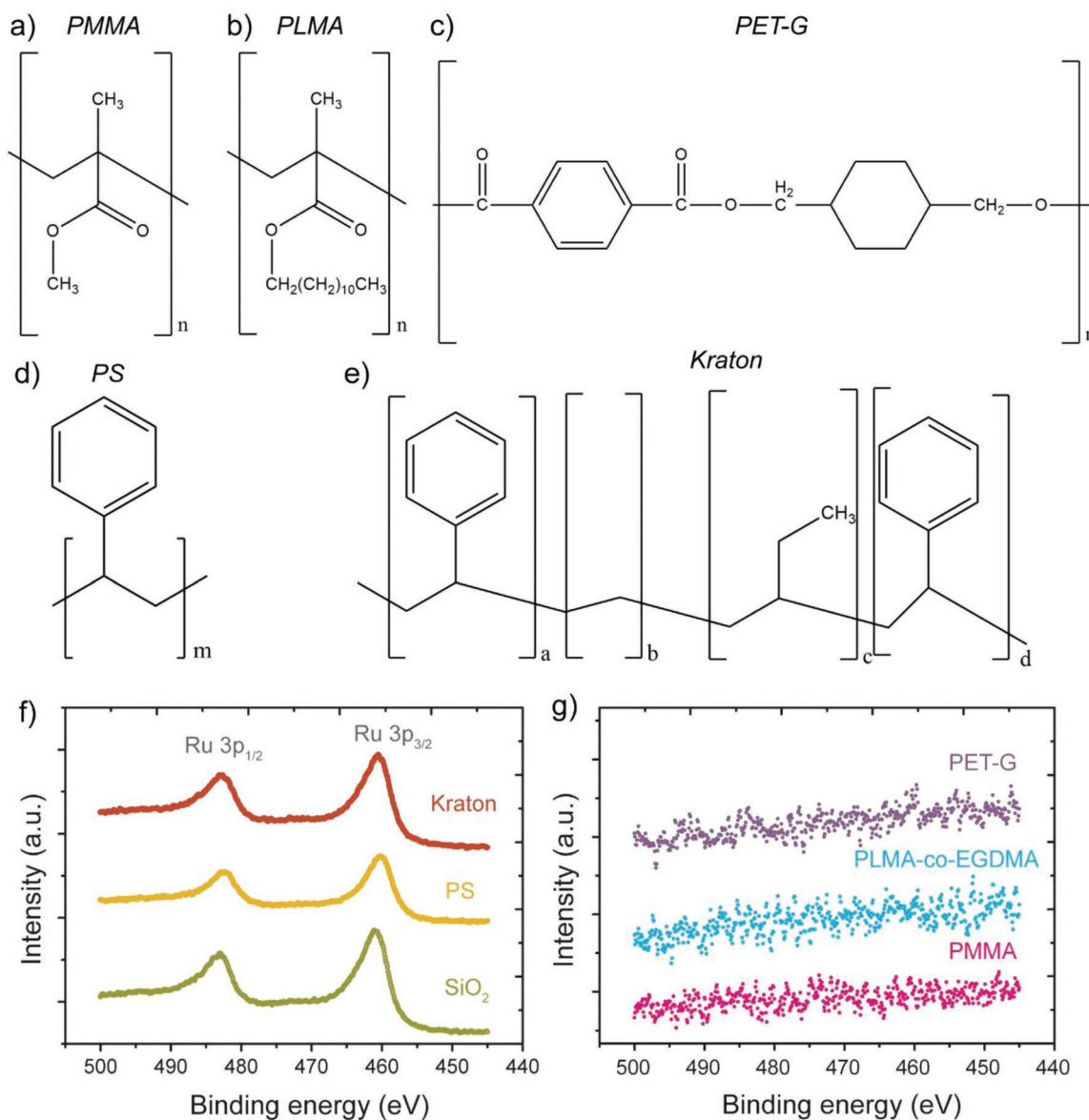


Figure 6. Chemical structures of different polymers studied. a) (Polymethyl methacrylate) PMMA, b) poly(lauryl methacrylate) PLMA, c) poly(ethylene terephthalate glycol) PET-G, d) (polystyrene) PS, and e) Kraton. f) Ru 3p XPS after 100 ALD cycles on kraton, PS, and SiO₂ and g) PMMA, PLMA-co-EGDMA, and PET-G. The XPS spectra have been given a vertical offset for clarity.

This in turn means that these polymers in Figure 6g can be used as mask layers for AS-ALD of RuO₂ further expanding the library of polymer based mask layers. Moreover, the fact that PMMA, PLMA, and PET-G contain a C=O functional group and PS and kraton contain aromatic C=C rings, provides a hint that polymers with C=O groups could act as best blocking layers for AS-ALD of RuO₂. Although, based on our data this is most likely the case, more in depth studies on this aspect are required to confirm the hypothesis.

2.6. Proof of Concept

AS-ALD was confirmed by performing the RuO₂ process on a patterned SiO₂/PMMA substrate (Figure 7a). 90 cycles of the process were performed at a substrate temperature of 100 °C.

Planar scanning electron microscopy (SEM)-energy dispersive X-ray (EDX) was used to examine this sample.^[57] The EDX line scan revealed no indication about the presence of Ru (Ru_L) in the regions containing PMMA, whereas the SiO₂ regions revealed a clear Ru signal. This indicates that area selective deposition on a patterned SiO₂/PMMA sample was successful. The next step is to remove the unreacted PMMA present in the patterned sample. We attempted to remove the PMMA layer using O₂ plasma but discovered that the Ru EDX signal (not shown) decreased after the O₂ plasma treatment, indicating the possible formation of volatile RuO₄ by the reaction of RuO₂ and O₂. As a result, in this case, we used acetone followed by isopropanol to remove the PMMA so that the RuO₂ content remained unchanged during the PMMA removal. The absence of a carbon (C_k) peak in the EDX scan in Figure 7b indicated that PMMA has been removed after the acetone wash. The Ru

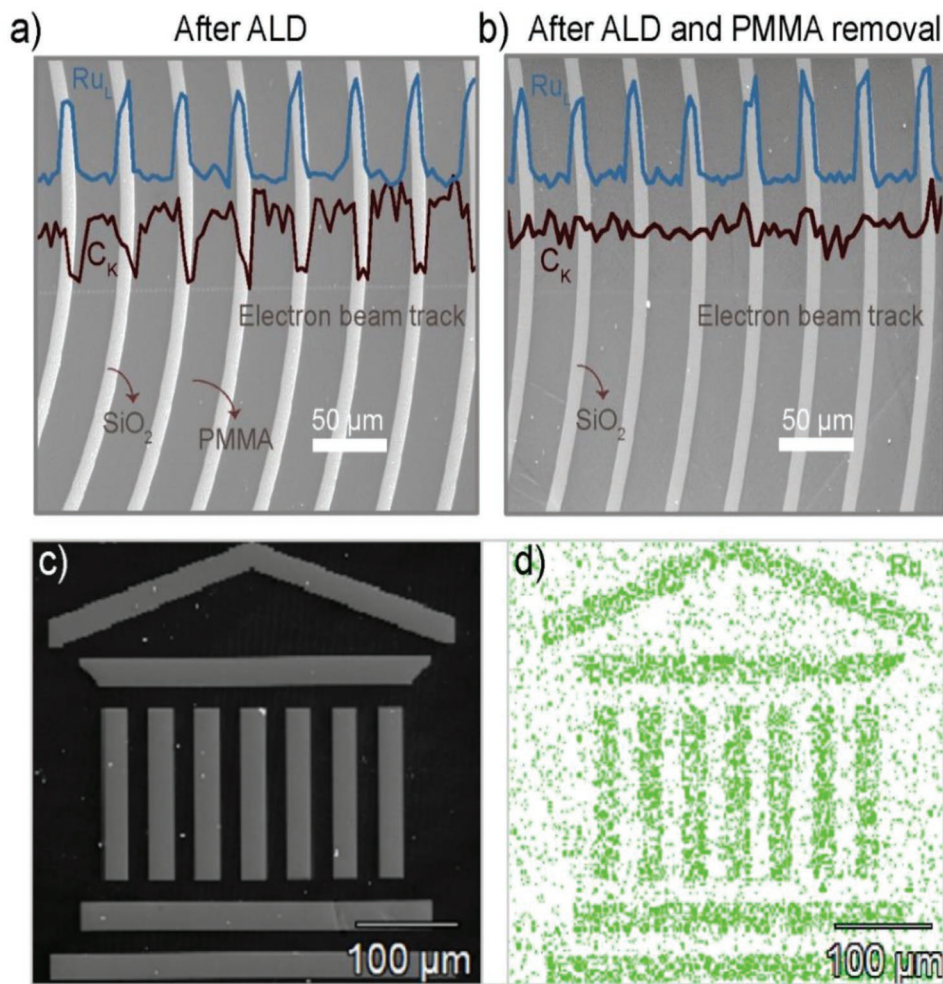


Figure 7. a) Planar view SEM images of patterned SiO₂/PMMA sample that was exposed to 90 methanol/RuO₄ ALD process. b) The same sample after removing PMMA by acetone treatment. The SEM images were taken after the EDX line scan was performed, perpendicular to the SiO₂ lines. The integrated EDX intensities of Ru and C peaks are also presented. c) A backscattered electron image of the logo of Ghent University with Si/PMMA patterns and d) the EDX elemental mapping of Ru for the sample in (c).

EDX intensities before and after the acetone dip were compared to see if any Ru was lost during the acetone dip. The Ru intensity appeared to be nearly the same in both cases, as shown in Figure S6 in the Supporting Information, indicating the stability of RuO₂ in acetone. In addition, SiO₂/PMMA patterns resembling the Ghent University (Belgium) logo were created, as shown in Figure 7c, and RuO₂ ALD was performed on this sample as well. The EDX mapping performed after the AS-ALD and acetone treatment on this sample confirms that the Ru is concentrated on the regions where there is SiO₂ and clearly establishes the process's selectivity once more.

2.7. Scanning Transmission Electron Microscopy (STEM)

Bright field (BF)-STEM analysis was used to confirm the selectivity of RuO₂ on patterned SiO₂/PMMA samples as well as to ensure that the PMMA layer is removed after the acetone treatment without affecting the RuO₂ layer next to it. Figure S7 in the Supporting Information depicts a cross-sectional BF-STEM image recorded immediately following AS-ALD on a SiO₂/PMMA

patterned sample and the EDX maps of relevant elements. The figure clearly shows that RuO₂ deposition occurred only on the SiO₂ region, whereas the PMMA region is clearly inert to RuO₂ deposition. Some degradation of PMMA can be observed near the SiO₂ region due to the ion milling preparation. This sample was then treated with acetone to remove the unreacted PMMA, and the resulting STEM and EDX images are shown in Figure 8. The uniformity of the RuO₂ layer on SiO₂ after removing the PMMA is clear. The STEM image and EDX maps for elemental carbon show that the PMMA has been completely removed from the sample. Furthermore, the RuO₂ layer appears to be unaffected by the acetone treatment. Based on this figure, ≈19–20 nm of RuO₂ was selectively deposited on the SiO₂ region.

3. Conclusion

In this work, we demonstrate that the methanol-RuO₄ ALD process to deposit RuO₂ has inherent substrate selectivity, facilitating RuO₂ deposition on SiO₂ while inhibiting growth on PMMA films. XRF, XPS, and STEM confirmed the selectivity,

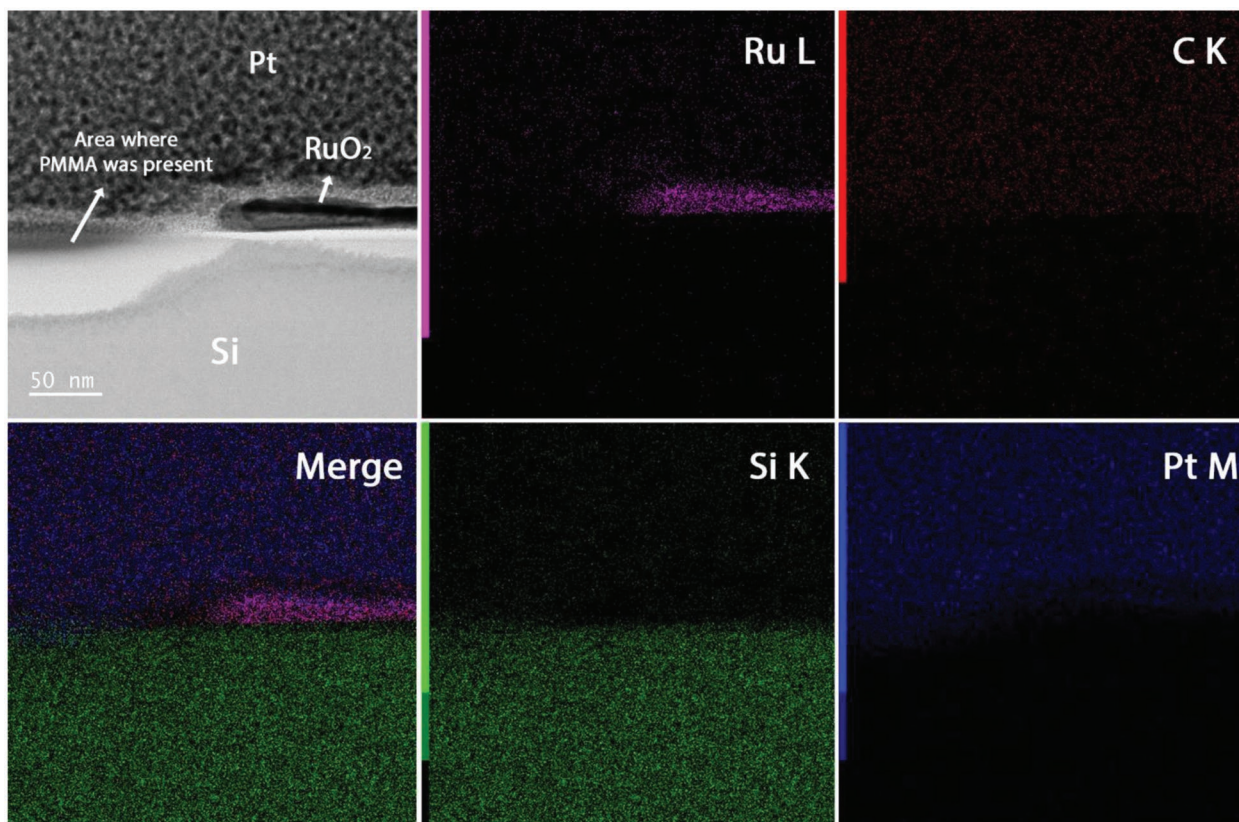


Figure 8. Cross-sectional BF-STEM image of the patterned SiO₂/PMMA sample after 90 ALD cycles with EDX maps of the samples after PMMA is removed.

while XRR measurements on SiO₂ revealed that ≈24 nm of RuO₂ can be selectively deposited on SiO₂. Since the deposition temperature has no effect on the process's selectivity, selective ALD was possible even at temperatures as low as 60 °C. We also discovered that the thickness of the PMMA layer used has no effect on selectivity. Interestingly, other alcohols, such as ethanol or 2-propanol, can be used to achieve similar selectivity, but with a higher growth of RuO₂ on SiO₂. Furthermore, the feasibility of PLMA-co-EGDMA, PET-G, PS, and Kraton as mask layers for AS-ALD of RuO₂ was investigated. We discovered that polymers with C=O in their structure, such as PLMA-co-EGDMA and PET-G, can be used as effective mask layers for the selective deposition of RuO₂, broadening the polymer subset that can be used for area selective processing in general. As a proof of concept, we demonstrated area selective ALD on patterned SiO₂/PMMA substrates. EDX and STEM measurements confirmed the selective deposition on such substrates. Finally, to obtain RuO₂ structures on SiO₂, a simple acetone wash is used to remove the unreacted PMMA part from the substrate. Based on the findings, we anticipate that the selective RuO₂ ALD will be applicable to other dielectrics and metals, enabling oxide on oxide or oxide on metal selective processing strategies.

4. Experimental Section

ALD Setup: The ALD was performed in a custom built high-vacuum ALD reactor with a base pressure of ≈10⁻⁶ mbar.^[49] A turbomolecular

pump in combination with a rotary vane backing pump are used to achieve this pressure. The chamber walls were heated to 90 °C to avoid precursor condensation. The precursors are kept inside stainless steel containers and are delivered to the reactor via stainless steel tubing.

Deposition Process: RuO₂ ALD was achieved by using RuO₄ and methanol as coreactants as reported before (please see this paper for the mechanism and ALD characteristics of the RuO₂ ALD process used here).^[48] RuO₄ was supplied to the reactor using the ToRuS precursor, which is a solution of RuO₄ in a methyl-ethyl fluorinated solvent developed and produced by Air Liquide.^[50] The ToRuS solution helps to alleviate the potential danger associated with the dealing of pure RuO₄, without compromising reactivity or vapor pressure. Experiments conducted by Air Liquide showed that the ToRuS solution was nontoxic, noncorrosive, and nonflammable. Most importantly no toxicity was reported as evidenced from their inhalation studies.^[50] Since the concentration of RuO₄ in the solution is very low (less than 1%), the potential danger is limited in case of spills. However, the use of personal protection equipment, including the use of respiratory protection methods (ABEK2 filters) was recommended. Methanol (99%) was purchased from Sigma-Aldrich. Both the precursors were kept at room temperature, whereas the stainless steel delivery lines were heated to 60 °C. During the methanol pulse and the RuO₄ pulse, the gate valve to the turbomolecular pump was kept opened, and the flow of the precursor gas through a needle valve caused the chamber pressure to increase to 7 × 10⁻³ mbar. The methanol and RuO₄ pulsing times were 25 and 40 s, respectively, and the pumping time for both was 50 s.

Substrate Preparation and PMMA Removal: All the PMMA samples were prepared by spin coating. Patterned Si/PMMA lines were obtained by first spin coating the PMMA layer on a Si with native oxide substrate. The e-beam/deep UV resist used was AR-P 617.06 manufactured by All-Resist. The resist is composed of copolymers based on polymethyl methacrylate and methacrylic acid (PMMA/MA = 33%). The solid

concentration is 6%. The solvent used for spin-coating is 1-methoxy-2-propanol. The hard baking was done in air. The acceleration rate for the spin coating was 1000 rpm s⁻¹.

The cleaning steps performed before spin coating the PMMA, were

1. The Si substrate with native oxide was first rinsed in an acetone bath for 1 min followed by a short rinse in isopropyl alcohol and then in deionized water.
2. After the rinse, the substrate was blow dried using a nitrogen gun and then a dehydration bake was performed on a hotplate at 120 °C for 2 min.
3. Finally, an O₂ plasma cleaning at 600 sccm of O₂ at 0.054 mbar was done for 10 min in a PVA Tepla plasma cleaning system.

The spin coating was performed for 60 s, with a spin speed of 4000 rpm and an acceleration of 1000 s⁻¹. The sample was baked at 250 °C for 2 min. This is followed by the spin coating of the photo resist, AZ5214E. (spin coating parameters; 4000 rpm, 1000 acceleration s⁻¹, time 40 s) (bake parameters; 100 °C, 3 min). The partial development of the resist was done using AZ400K: water (1:3) for 15 s. Following this, dry etch in O₂ RIE is performed to obtain the patterns. Finally, the photoresist is removed using acetone and water rinse. This synthesis procedure of the patterned samples is schematically demonstrated in Figure S5 in the Supporting Information. After the AS-ALD, the PMMA regions were removed by dipping the sample in hot acetone (60 °C) for about 5 min.

Material and Process Characterization: XRF was performed using a Bruker Artax system comprising a Mo X-ray source and an XFlash 5010 silicon drift detector and each measurement lasted for 100 s. RuO₂ film thicknesses were determined from XRR. XRR and X-ray diffraction (XRD) were carried out using a Bruker D8 system with Cu K_α radiation. The XRD measurements were performed in theta–2theta geometry. PMMA thin film thicknesses were obtained using a Woollam M-2000 spectroscopic ellipsometer. XPS measurements were performed on a Thermo Scientific Theta Probe XPS instrument using Al K_α (λ = 0.834 nm) X-rays generated at 15 kV and 70 W and focused to a spot size of 0.3 mm by an MXR1 monochromator gun. Ru 3p peaks were analyzed because of the overlap of Ru 3d with C 1s.

Area-selective RuO₂ deposition on patterned Si/PMMA substrates was evaluated by SEM and STEM with BF detector and operated at JEOL 2200FS with 200 kV. The composition was determined via EDX spectroscopy in BF-STEM mode. Cross-sectional STEM lamella was prepared using ion milling techniques via the focused ion beam in situ lift-out procedure. The protective layer Pt was deposited to protect the lamella during the ion preparation. SEM was performed using an field emission gun (FEG) Quanta 200 F instrument, combined with a silicon drift detector to perform EDX spectroscopy. EDX line scan and EDX mapping were performed at a beam energy of 10 keV.

Supporting Information

Supporting Information is available from the Wiley Online Library or from the author.

Acknowledgements

This project has received funding from the European Union's Horizon 2020 research and innovation programme under the Marie Skłodowska-Curie grant agreement no. 765378. H.R. acknowledges support and funding as postdoctoral fellow fundamental research of the Research Foundation – Flanders (FWO) under grant number 1273621N.

Conflict of Interest

The authors declare no conflict of interest.

Author Contributions

The paper was written through contributions of all authors. All authors have given approval to the final version of the paper.

Data Availability Statement

The data that support the findings of this study are available from the corresponding author upon reasonable request.

Keywords

area-selective deposition, chemical vapor deposition, patterning, PMMA, polystyrene

Received: August 31, 2022

Revised: November 8, 2022

Published online:

- [1] H. Over, Y. D. Kim, A. Seitsonen, S. Wendt, E. Lundgren, M. Schmid, P. Varga, A. Morgante, G. Ertl, *Science* **2000**, 287, 1474.
- [2] S. Trasatti, *Electrochim. Acta* **2000**, 45, 2377.
- [3] H. Over, *Chem. Rev.* **2012**, 112, 3356.
- [4] K. Fröhlich, K. Husekova, D. Machajdik, J. Hooker, N. Perez, M. Fanciulli, S. Ferrari, C. Wiemer, A. Dimoulas, G. Vellianitis, *Mater. Sci. Eng., B* **2004**, 109, 117.
- [5] M. Hasan, H. Park, J.-M. Lee, H. Hwang, *Appl. Phys. Lett.* **2007**, 91, 033512.
- [6] S. Y. Kang, C. S. Hwang, H. J. Kim, *J. Electrochem. Soc.* **2005**, 152, C15.
- [7] S.-S. Yim, D.-J. Lee, K.-S. Kim, M.-S. Lee, S.-H. Kim, K.-B. Kim, *Electrochem. Solid-State Lett.* **2008**, 11, K89.
- [8] S. Saito, K. Kuramasu, *Jpn. J. Appl. Phys.* **1992**, 31, 135.
- [9] Y. H. Kim, M. Kim, Y. Kotsugi, T. Cheon, D. Mohapatra, Y. Jang, J. S. Bae, T. E. Hong, R. Ramesh, K. S. An, *Adv. Funct. Mater.* **2022**, 32, 2206667.
- [10] S. M. George, *Chem. Rev.* **2010**, 110, 111.
- [11] R. W. Johnson, A. Hultqvist, S. F. Bent, *Mater. Today* **2014**, 17, 236.
- [12] M. Ritala, M. Leskela, in *Handbook of Thin Films Materials*, Vol. 1, Academic Press, UK **2002**, pp. 103–159.
- [13] V. Cremers, R. L. Puurunen, J. Dendooven, *Appl. Phys. Rev.* **2019**, 6, 021302.
- [14] C. Detavernier, J. Dendooven, S. P. Sree, K. F. Ludwig, J. A. Martens, *Chem. Soc. Rev.* **2011**, 40, 5242.
- [15] M. F. Vos, S. N. Chopra, M. A. Verheijen, J. G. Ekerdt, S. Agarwal, W. M. Kessels, A. J. Mackus, *Chem. Mater.* **2019**, 31, 3878.
- [16] A. J. Mackus, M. J. Merckx, W. M. Kessels, *Chem. Mater.* **2018**, 31, 2.
- [17] N. P. Dasgupta, H.-B.-R. Lee, S. F. Bent, P. S. Weiss, *Chem. Mater.* **2016**, 28, 1943.
- [18] A. Mameli, Y. Kuang, M. Aghaee, C. K. Ande, B. Karasulu, M. Creatore, A. J. Mackus, W. M. Kessels, F. Roozeboom, *Chem. Mater.* **2017**, 29, 921.
- [19] S. E. Atanasov, B. Kalanyan, G. N. Parsons, *J. Vac. Sci. Technol., A* **2016**, 34, 01A148.
- [20] J. Kwon, M. Saly, M. D. Halls, R. K. Kanjolia, Y. J. Chabal, *Chem. Mater.* **2012**, 24, 1025.
- [21] G. N. Parsons, R. D. Clark, *Chem. Mater.* **2020**, 32, 4920.
- [22] M. J. Weber, A. J. Mackus, M. A. Verheijen, C. van der Marel, W. M. Kessels, *Chem. Mater.* **2012**, 24, 2973.
- [23] J. A. Singh, N. F. Thissen, W.-H. Kim, H. Johnson, W. M. Kessels, A. A. Bol, S. F. Bent, A. J. Mackus, *Chem. Mater.* **2018**, 30, 663.

- [24] A. J. Mackus, M. J. Weber, N. F. Thissen, D. Garcia-Alonso, R. H. Vervuurt, S. Assali, A. A. Bol, M. A. Verheijen, W. M. Kessels, *Nanotechnology* **2015**, *27*, 034001.
- [25] E. K. Seo, J. W. Lee, H. M. Sung-Suh, M. M. Sung, *Chem. Mater.* **2004**, *16*, 1878.
- [26] F. S. Minaye Hashemi, B. R. Birchansky, S. F. Bent, *ACS Appl. Mater. Interfaces* **2016**, *8*, 33264.
- [27] E. Färm, M. Kemell, M. Ritala, M. Leskelä, *Thin Solid Films* **2008**, *517*, 972.
- [28] W. Lee, F. B. Prinz, *J. Electrochem. Soc.* **2009**, *156*, G125.
- [29] H.-B.-R. Lee, M. N. Mullings, X. Jiang, B. M. Clemens, S. F. Bent, *Chem. Mater.* **2012**, *24*, 4051.
- [30] S. N. Chopra, Z. Zhang, C. Kaihlanen, J. G. Ekerdt, *Chem. Mater.* **2016**, *28*, 4928.
- [31] X. Yu, D. Bobb-Semple, I.-K. Oh, T.-L. Liu, R. G. Closser, W. Trevillyan, S. F. Bent, *Chem. Mater.* **2021**, *33*, 902.
- [32] T.-L. Liu, S. F. Bent, *Chem. Mater.* **2021**, *33*, 513.
- [33] A. Mameli, M. J. Merckx, B. Karasulu, F. Roozeboom, W. M. Kessels, A. J. Mackus, *ACS Nano* **2017**, *11*, 9303.
- [34] M. J. Merckx, S. Vlaanderen, T. Faraz, M. A. Verheijen, W. M. Kessels, A. J. Mackus, *Chem. Mater.* **2020**, *32*, 7788.
- [35] J. Yarbrough, A. B. Shearer, S. F. Bent, *J. Vac. Sci. Technol., A* **2021**, *39*, 021002.
- [36] R. Khan, B. Shong, B. G. Ko, J. K. Lee, H. Lee, J. Y. Park, I.-K. Oh, S. S. Raya, H. M. Hong, K.-B. Chung, *Chem. Mater.* **2018**, *30*, 7603.
- [37] H. G. Kim, M. Kim, B. Gu, M. R. Khan, B. G. Ko, S. Yasmeen, C. S. Kim, S.-H. Kwon, J. Kim, J. Kwon, *Chem. Mater.* **2020**, *32*, 8921.
- [38] A. Mackus, A. Bol, W. Kessels, *Nanoscale* **2014**, *6*, 10941.
- [39] S. S. Vandembroucke, M. Nisula, R. Petit, R. Vos, K. Jans, P. M. Vereecken, J. Dendooven, C. Detavernier, *Langmuir* **2021**, *37*, 12608.
- [40] T.-L. Liu, L. Zeng, K. L. Nardi, D. M. Hausmann, S. F. Bent, *Langmuir* **2021**, *37*, 11637.
- [41] E. Färm, M. Kemell, M. Ritala, M. Leskelä, *J. Phys. Chem. C* **2008**, *112*, 15791.
- [42] A. Sinha, D. W. Hess, C. L. Henderson, *J. Electrochem. Soc.* **2006**, *153*, G465.
- [43] J. Hong, D. W. Porter, R. Sreenivasan, P. C. McIntyre, S. F. Bent, *Langmuir* **2007**, *23*, 1160.
- [44] A. Haider, M. Yilmaz, P. Deminskyi, H. Eren, N. Biyikli, *RSC Adv.* **2016**, *6*, 106109.
- [45] N. Biyikli, A. Haider, P. Deminskyi, M. Yilmaz, in *Low-Dimensional Materials and Devices 2017*, Vol. 10349, Event: SPIE Nanoscience Engineering, San Diego, California, USA **2017**, p. 103490M, <https://doi.org/10.1117/12.2276141>.
- [46] E. Färm, M. Kemell, E. Santala, M. Ritala, M. Leskelä, *J. Electrochem. Soc.* **2010**, *157*, K10.
- [47] T. Aaltonen, A. Rahtu, M. Ritala, M. Leskelä, *Electrochem. Solid-State Lett.* **2003**, *6*, C130.
- [48] N. Poonkottil, M. M. Minjauw, A. Werbrouck, S. Checchia, E. Solano, M. Nisula, A. Franquet, C. Detavernier, J. Dendooven, *Chem. Mater.* **2022**, *34*, 8946.
- [49] J. Musschoot, Q. Xie, D. Deduytsche, S. Van den Berghe, R. Van Meirhaeghe, C. Detavernier, *Microelectron. Eng.* **2009**, *86*, 72.
- [50] J. Gatineau, K. Yanagita, C. Dussarrat, *Microelectron. Eng.* **2006**, *83*, 2248.
- [51] W. L. Gladfelter, *Chem. Mater.* **1993**, *5*, 1372.
- [52] A. Mameli, B. Karasulu, M. A. Verheijen, B. Barcones, B. Macco, A. J. Mackus, W. M. E. Kessels, F. Roozeboom, *Chem. Mater.* **2019**, *31*, 1250.
- [53] M. M. Minjauw, J. Dendooven, B. Capon, M. Schaeckers, C. Detavernier, *J. Mater. Chem. C* **2015**, *3*, 132.
- [54] M. Pasquali, P. Carolan, S. Sergeant, J. Meersschaut, V. Spampinato, T. Conard, A. Viva, S. De Gendt, S. Armini, *ACS Appl. Electron. Mater.* **2022**, *4*, 1703.
- [55] T. H. Cho, N. Farjam, C. R. Allemang, C. P. Pannier, E. Kazyak, C. Huber, M. Rose, O. Trejo, R. L. Peterson, K. Barton, *ACS Nano* **2020**, *14*, 17262.
- [56] A. Sinha, D. W. Hess, C. L. Henderson, *J. Vac. Sci. Technol., B: Microelectron. Nanometer Struct.–Process., Meas., Phenom.* **2006**, *24*, 2523.
- [57] W. Li, P. F. Smet, L. I. Martin, C. Pritzel, J. S. auf der Günne, *Phys. Chem. Chem. Phys.* **2020**, *22*, 818.